Magnetic Waves for Microwave Time Delay—Some Observations and Results

I. KAUFMAN, SENIOR MEMBER, IEEE, AND R. F. SOOHOO, SENIOR MEMBER, IEEE

Abstract—Some topics of exchange-coupled spin waves and magnetostatic waves in narrow line width ferrimagnetic materials for electronically variable time delay of microwave signals in the microsecond realm are discussed. The excitation problem is treated by use of transmission-line analogs. A method of excitation of spin waves by microscopic geometries is suggested, and an estimate of its efficiency given.

Results of experiments of magnetic wave excitation in axially magnetized YIG rods are presented. Here very strong excitation of signals with high dispersion and microsecond time delay that is a sensitive function of H_{dc} were found. These signals possess most of the characteristics predicted for Fletcher-Kittel waves. Other signals, with less dispersion and a much more slowly variable time delay, were also found.

I. Introduction

RECENTLY interest has arisen in compact systems for microsecond time delay of microwave signals. This paper discusses some topics related to wave propagation in ferrimagnetic materials for performing such time-delay functions.

Acoustic waves and some magnetic waves possess the the property of very low velocities—about five orders of magnitude below electromagnetic speeds. This property reduces the length of a microsecond delay line from thousands of meters to centimeters.

In acoustic wave propagation, the velocity of a signal is nearly constant. In magnetic wave propagation, on the other hand, where the energy of the electron spin system that propagates the wave is a strong function of the dc magnetic field, small changes in H_{dc} can cause a large change in the velocity of propagation. Magnetic wave delay lines, therefore, can have wide ranges of electronically variable delay.

It is possible in some magnetic materials to effect a conversion between acoustic and magnetic waves. Methods of using these combined "magnetoelastic" waves for time-delay devices have recently been described [1], [2]. In this paper, we shall deal principally with waves in magnetic form.

The most perceptible difference between the magnetic waves considered here and those commonly used in ferrite phase shifters is their difference in velocity. Both are essentially "waveguide" transmission systems. However, the electrical length of the phase shifter is only of the order of a few wavelengths, so that even a lossy ferrite will not attenuate a wave appreciably. The electrical length of a spin-wave microsecond delay line, on the other hand, is thousands of wavelengths; so that a low-loss material, such as single-crystal YIG, is required.

Manuscript received December 8, 1964; revised March 31, 1965.

I. Kaufman is at Centro Microonde, Florence, Italy. He is on leave of absence from TRW Space Technology Labs., Redondo Beach, Calif.

R. F. Soohoo is with the University of California, Davis, Calif. He is a Consultant to TRW Space Technology Labs.

II. Magnetic Waves

A. Plane Waves

Electromagnetic plane waves in ferrimagnetic materials propagate with a velocity that is of the order of c. However, because of the anisotropic nature of these materials, electromagnetic wave types can exist that exhibit a dispersion. B. A. Auld [3] has shown that when some of these dispersive waves are plotted on an ω-k diagram, they join smoothly to waves of lower phase and group velocities, the magnetostatic waves. Finally, the curves describing the latter join smoothly to the waves that arise because of "exchange" coupling, the so-called "spin waves."

The particular form of wave that can exist in a material, i.e., electromagnetic, magnetostatic, or spin wave, depends on the dc magnetic field H_{dc}. Since each region is characterized by different wave velocities, we can see that a change of H_{dc} will change the wave speed.

For microsecond delays in small specimens, we are particularly interested in the spin-wave region. Here, the dispersion relation is that of the well-known spin-wave manifold [4], [5]

$$\omega_k = [|\gamma| H_i + (|\gamma| 2A/M_s)k^2]^{1/2} \cdot [|\gamma| H_i + (|\gamma| 2A/M_s)k^2 + \omega_M \sin^2\theta_k]^{1/2}. \quad (1)$$

For (1), the usual convention of a z-directed H_{dc} (here of value H_i) is used. A is the exchange constant of the material; ω_k is the spin-wave angular frequency; γ is the gyromagnetic constant; M_s is the magnetization; k is the wave vector; $\omega_M = 4\pi|\gamma| M_s$; and θ_k is the angle between the z axis and the direction of k.

To demonstrate the use of spin waves for electronically variable time delay, we can consider the simple case of $\theta_k = 0$. Then, $\omega_k = |\gamma|(H_i + 2Ak^2/M_s)$, so that we get a group velocity v_g of

$$v_g = \frac{\partial\omega_k}{\partial k} = \frac{4kA}{M_s} = 2|\gamma|\left(\frac{2A}{M_s}\right)^{1/2}\left(\frac{\omega_k}{|\gamma|} - H_i\right)^{1/2}. \quad (2)$$

A parcel of energy contained in a microwave pulse of center frequency ω_k would propagate in such a spin system with a velocity given by (2). We note that v_g varies with H_i. For $H_i > \omega_k/|\gamma|$ there is no propagation; below this, propagation occurs. For room temperature YIG, and at 3000 Mc, v_g can be made to vary from zero to the maximum value of $2|\gamma|(2A/M_s)^{1/2}(\omega_k/|\gamma|)^{1/2} = (9.65)(10^4)$ cm/s, merely by decreasing the internal dc magnetic field from 1070 oersteds (Oe) to zero. Thus, we would be able to vary the propagation time per centimeter length of material from 10.3 μs to infinity.

B. Effect of Boundary Conditions

In addition to plane wave propagation at low velocities, there exists the possibility of energy propagation by slow waves governed by boundary conditions. These magnetostatic waves obey, approximately, the relation $\nabla \times \boldsymbol{h} = 0$ inside a specimen. The matching at the boundary of the fields inside a specimen with those that can exist outside then determines the allowed wave field distributions and velocities.

This method has been applied by several workers [6]–[8]. Of particular interest to us here are the modes found by Fletcher and Kittel [7], who predicted the feasibility of very slow magnetostatic waves in long magnetized cylinders.[1] They arrived at the relation between frequency and wave number of

$$\omega \simeq |\gamma| H_i + 2\pi |\gamma| M_s(2.405/kR)^2, \qquad (3)$$

where H_i is the longitudinal dc field in the rod and R, is the radius.

To take into account the fact that the very short wavelength spin waves governed by (1) could also exist in these cylinders (almost independent of the boundaries), Fletcher and Kittel added a term for these waves to the dispersion relation, resulting in

$$\omega \simeq |\gamma| H_i + 2\pi |\gamma| M_s(2.405/kR)^2 + |\gamma| (2A/M_s)k^2. \qquad (4)$$

Figure 1 is plot of (4) for a rod of room temperature YIG. Here the region on the left corresponds to the Fletcher-Kittel mode, i.e., the last term of (3); the region on the right is the spin-wave region, i.e., the last term of (4). The shift from curve to curve is due to the $|\gamma| H_i$ term, which is present in both (1) and (3), and, therefore, in (4).

Of interest is the manner in which the group velocity in such a rod changes as H_{dc} is varied, while the signal frequency remains constant. This is shown in Fig. 2. Here absolute values of v_g have been plotted, since the Fletcher-Kittel mode of (3), hereafter referred to as F-K mode, is a backward-wave mode.[2]

[1] Note added in proof: This problem has also been treated elsewhere. See, Joseph, R. I., and E. Schlomann, Theory of magnetostatic modes in long, axially magnetized cylinders, *J. Appl. Phys.*, vol 32, Jun 1961, pp 1001–1005.

[2] Backward-wave modes were also found by Damon and Eshbach [8].

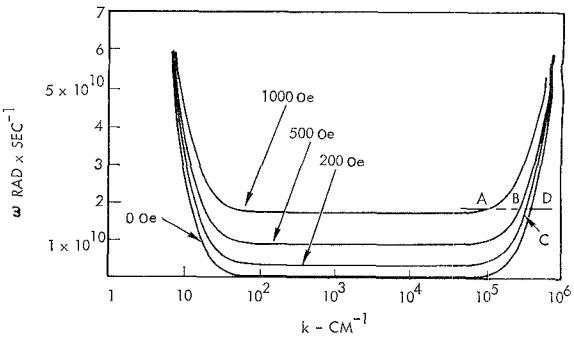

Fig. 1. Dispersion diagram (ω vs. k) for magnetic wave propagation in a longitudinally magnetized cylinder of YIG (room temperature, where $4\pi M_0 \simeq 1750$ Oe) of radius 0.19 cm, for various values of H_{dc}.

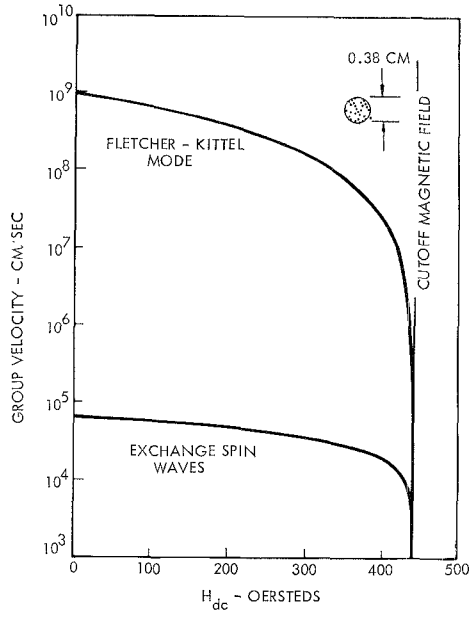

Fig. 2. Group velocity vs. H_{dc}, for exchange spin waves and for Fletcher-Kittel magnetostatic waves. Room temperature YIG. Frequency: 1230 Mc.

We note the following:

1) At a given frequency ω, both F-K and spin-wave modes exist only below the resonance field, where $H_i = \omega/|\gamma|$.

2) Both modes have electronically variable delay characteristics. In both cases, in the region below $\omega/|\gamma|$, an increase in H_i results in a reduction of group velocity and, therefore, in an increase in time delay.

3) At low values of H_i, the F-K mode reverts to propagation at electromagnetic speeds; the exchange mode does not. This means that the F-K mode could be used for time delays of from nanoseconds per centimeter of length of material up to microseconds per centimeter; the exchange mode has a minimum delay of several microseconds per centimeter. At 1230 Mc, for example, this minimum rate is 16 μs/cm.

4) Because the F-K mode is so highly variable in group velocity, it will be characterized by very narrow bandwidths when used for delay rates in the microseconds per centimeter range. On the other hand, it should have a considerably wider bandwidth when used for delay rates in the nanoseconds per centimeter range.

III. Excitation

In Section II, we have sketched the behavior of some magnetic slow waves. In the present section, we will discuss their excitation. Some aspects of coherent spin-wave excitation have been treated previously, principally from a mathematical point of view [9]–[11]. We suggest here a transmission-line analog, which leads us to suggest a new method for wave excitation. Finally, we conclude the section by examining the applicability of the "Net Dipole Moment" technique, discovered by Schlömann [9], to F-K wave excitation.

A. Transmission Line Analog

In the excitation of waveguides with probes, the exciter is usually smaller than the wavelength. Quite the opposite is true for spin-wave excitation. For example, for 1230 Mc exchange-type spin waves of delay rate 16 μs/cm, the guide wavelength $2\pi/k$ is $(2.5)(10^{-5})$ cm. This is about six orders of magnitude shorter than the electromagnetic wavelength at 1230 Mc. We have, therefore, the situation of an excitation field that is distributed over many wavelengths.

For coupling to spin waves with an RF magnetic field intensity, the equation of motion of a magnetization excited by a circularly polarized RF magnetic field, for a ferrimagnetic specimen with z-directed internal dc field, is [10]

$$\frac{d^2m_0}{dz^2} + \frac{\omega M_s}{2A|\gamma|}\left[\frac{-|\gamma|H_i}{\omega} + 1\right]m_0 = -\frac{M_s^2}{2A}h_0, \quad (5)$$

where M_s and m_0 are the dc and RF magnetizations, respectively, and all quantities are assumed to vary as $\exp(j\omega t)$. This is of the form of the differential equation for voltage along a parallel wire line excited by a distributed shunt current $J(\xi)e^{j\omega t}$, as in Fig. 3. The voltage along this transmission line is given by

$$d^2V/dz^2 + k^2V = -jkZ_0J, \quad (6)$$

where $k = 2\pi/\lambda$: Z_0 is the characteristic impedance.

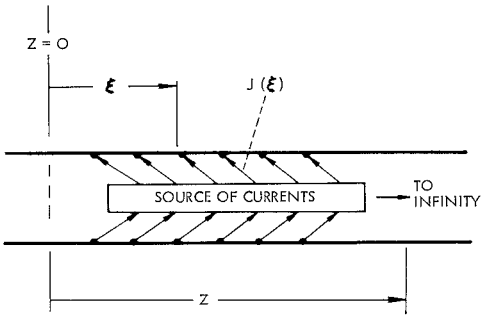

Fig. 3. Transmission line excited by distributed shunt current.

For a line short-circuited at $z=0$, the voltage developed at a point z by an incremental current $(J\zeta)d\xi$ flowing into the line at a point ξ between the origin and z is $jJZ_0(\sin k\xi)\exp(-jkz)d\xi$. The voltage developed by the current for the short-circuited case is, therefore,

$$V(z) = \exp(-jkz)\int_0^{\xi_{max}} Z_0J(\xi)(\sin k\xi)d\xi. \quad (7)$$

For the line that is open-circuited at $z=0$, the quantity $(\sin k\xi)$ is replaced by $(\cos k\xi)$.

Several special cases are of interest:

1) *Uniform Excitation Extending toward Infinity:* We assume here[3] that $J(\xi) = J_0e^{-K\xi}$, where K is vanishingly small. For uniform excitation, with linear current density J_0, we get:

a) With a short circuit at $z=0$,

$$V(z) \simeq (J_0Z_0/k)[\exp(-jkz)];$$

b) With an open circuit at $z=0$,

$$V(z) \simeq (J_0Z_0/k)(K/k)[\exp(-jkz)] \simeq 0. \quad (8)$$

2) *Uniform Excitation J_0 Extending to Finite Distance a:*

a) With a short circuit at $z=0$,

$$|V(z)| \simeq (J_0Z_0/k)|\cos ka - 1|;$$

b) With an open circuit at $z=0$,

$$|V(z)| \simeq (J_0Z_0/k)|\sin ka|. \quad (9)$$

3) *Concentrated Current $I_0 = (J_0)(a)$ Injected at $\xi = \lambda/4$:*

a) With a short circuit at $z=0$, $|V(z)| = J_0aZ_0$;

b) With an open circuit at $z=0$, $|V(z)| = 0$. (10)

The results of this simple analog can be applied to the case of spin-wave excitation, using the analogies of Table I.

TABLE I

Parallel Wire Transmission Line—Spin-Wave Analogies

Transmission Line	Spin Waves
V	m_0
k	$k=[(\omega M_s/2A\|\gamma\|)(-\|\gamma\|H_i/\omega+1)]^{1/2}$
$jkJZ_0$	$-M_0^2h_0/2A$

Since in the transmission-line case the short circuit is a point of zero voltage, the spin-wave equivalent is the plane of zero RF magnetization, i.e., the spins "pinned" condition. The analog of the electrical open circuit, accordingly, is the case of maximum spin precession, where $dm_0/dz = 0$.

If the RF h field, into which a specimen with an optically polished front surface is immersed, is uniform, then from (8) a wave can be generated at the front surface. For the spins "pinned" condition, this wave will be of amplitude $M_s^2h_0/2Ak^2$. For the boundary condition

[3] This form was used by Jacobsen [12] for computing the excitation at the free end of a piezoelectric crystal.

of $dm_0/dz=0$, however, the generated wave is of negligible amplitude.

To estimate the efficiency of conversion from an electromagnetic field to spin-wave energy for the spins "pinned" condition at a flat surface, we consider Fig. 4. Here we have a short-circuited coaxial transmission line with a rod of YIG inserted into a hole drilled in the short-circuiting plate. Although the internal fields are not equal to those applied and are not uniform across the specimen, we assume, for simplicity's sake, that the exciting field is that existing in an unperturbed short-circuited coaxial line at an average radius r_m (see Fig. 4). For such a line, the input power P_{in} into a matched load would be $I_m^2 Z_l/2$, where Z_l is the line impedance and I_m is the peak RF current. For our standing wave case, therefore we have $I_m=2[2P_{\text{in}}/Z_l]^{1/2}$. The magnetic field at r_m (in oersteds) is

$$h = [0.2/r_{m\text{cm}}][2(2P_{\text{in}}/Z_l)^{1/2}].$$

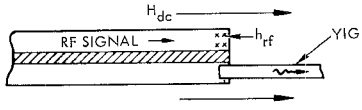

Fig. 4. Specimen of YIG inserted into hole of a wall terminating a coaxial transmission line. Here a cross section of YIG of dimensions $r_m \times r_m$ is assumed, with r_m the mean radius of the space between inner and outer conductors.

Since only one of the circular polarized components of the field excites spin waves, the effective excitation field is half of this amount. For the spin's "pinned" condition, we find, from the analogy shown, that $m_0 = M_s^2 h_{0\text{-oersteds}}/2Ak^2$. The power density associated with spin-wave propagation [10] is

$$p_{\text{ergs/cm}^2} = 2Ak\omega \frac{m_0^2}{M_s^2}.$$

Substituting, converting to watts, and multiplying by the area of the YIG, we find the following result:

$$P_{\text{watts}} = 10^{-9}\omega M_s^2 P_{\text{in}}/Ak^3 Z_l. \tag{11}$$

Inserting numerical values of $\omega=(2\pi)(3)(10^9)$ sec^{-1}; $M_s=192$ Oe; $k=(7.3)(10^4)$ cm^{-1}; and $A=(4.9)(10^{-7})$, we find that the coupled power is 37 dB below the power incident from the coaxial line. If the coaxial system is made resonant, the efficiency (for narrow-band coupling) is improved. However, better methods of coupling exist and are described later.

B. Excitation by Conductors of Microscopic Geometries

The weak conversion obtained from the configuration leading to (11) is due to the cancellation from alternate half wavelengths in the distributed excitation. While the usual microwave fields are distributed, it is also possible to get highly localized fields. An example is the very fine wire of a microwave bolometer, which can have very high fields in its immediate vicinity, dropping off quite rapidly with distance. We now consider excitation by such a wire, adjacent to a slab of ferrimagnetic material.

Accordingly, we estimate the amount of spin-wave excitation with the geometry of Fig. 5(a). Although such a system would naturally excite cylindrical waves, we will estimate the degree of coupling with the equivalent slab system of Fig. 5(b).

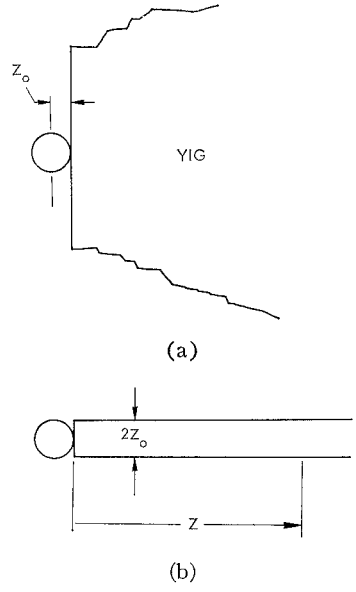

Fig. 5. Fine wire carrying RF current placed adjacent to polished YIG surface. (a) Actual configuration. (b) Slab line approximation used in calculations.

We will further assume that the field in the YIG is that surrounding a current-carrying wire in free space and that the coupled power is of the order of magnitude that would be coupled to a spin-wave "transmission line" of a width equal to the wire diameter.

The equation to be solved here is

$$d^2m_0/dz^2 + k^2 m_0 = D_0/(z+z_0), \tag{12}$$

where $D_0=(-M_s^2/2A)(0.1)(I_{\text{amp}})$. (As before, only half of the h field of the wire is effective in coupling to the circularly polarized spin waves.) The solution to (12) depends on the boundary conditions at the surface of the slab. We consider here the two cases of spins pinned and unpinned.

1) *Spins Pinned at Slab Surface:* For this case ($m_0=0$ at $z=0$), the solution of (12) for large z is

$$m_0 = -\{D_0/k\}\left\{\text{Ci}(kz_0)\sin kz_0 + \left[\frac{\pi}{2} - \text{Si}(kz_0)\right]\cos kz_0\right\}\{\exp(-ikz)\}$$
$$\simeq (M_s^2)(0.1)(I_{\text{amp}})/2Ak(kz_0), \tag{13}$$

where *Ci* and *Si* are the sine and cosine integrals. For the strip of height $2z_0$ and width L, the transmitted spin-wave power, thus, becomes

$$P_{\text{watts}} = (10^{-9})\omega M_s^2 I_{\text{amp}}^2 (2z_0)(L)/2Ak(kz_0)^2. \tag{14}$$

A crucial quantity is the radius of the wire z_0. For a 34-microinch platinum wire, as used in X-band bolometers, coupling to 3000-Mc spin waves of a 34-microinch wavelength (requiring a magnetic field of 1044 Oe and resulting in a group velocity of 0.013 cm/μs), with $A=(4.9)(10^{-7})$ ergs/cm and $L=0.5$ cm, we find

$$P_{\text{watts-spin}} = 43 I_{\text{amp}}^2. \tag{15}$$

At room temperature, where the resistivity of platinum is 10^{-5} Ω/cm, the resistance of our wire is 860 Ω. Such a wire can be made to absorb all of the power P_g passing through a waveguide. (This is what happens in the use of a bolometer.) In that case, the current through the wire is $I_{\text{amp}}=(2P_g/860)^{1/2}$. With this wire placed next to an optically polished specimen of YIG, the ratio of coupled spin-wave power to waveguide power is 1/10. At a lower temperature, where the resistance of platinum is less, the coupling should increase. It appears, therefore, that this method of coupling could be successful.

2) *Maximum Spin Procession at Surface:* Here we find a less favorable case. For large z, the spin-wave amplitude is found to be given by

$$m_0 \simeq (M_s^2)(0.1)(I_{\text{amp}})/2Ak(kz_0)^2. \tag{16}$$

Because of the extra (kz_0), this case results in much smaller coupling than the spins "pinned" case. This situation is also readily seen by looking at the transmission-line analog.

We conclude from these estimates that, if the spins "pinned" condition were the true surface condition, the method of an ultrafine wire or an evaporated filament of conductive material could be an efficient way of converting electromagnetic waves to spin waves. Unfortunately, there are some drawbacks. A separate calculation for Case 1), previously mentioned, demonstrates that this coupling would be restricted to low-power levels. There, with a limiting precession angle of 5° at the YIG surface, the power level in the YIG would be $(2)(10^{-5})$ watts. Furthermore, the waves generated would be cylindrical waves, so that it would be necessary to use highly accurate semicylindrical structures to detect them. However, it might be possible to utilize the dispersive nature of the material for focusing, or to use multiple excitation structures, such as gratings.

C. The Method of Net Dipole Moment

This method has been discussed in detail by Schlömann [9], [10]. In this section, we present only a microwave analog. In Section III-D, we examine the applicability of the technique to the excitation of F-K waves.

As seen in Section III-A, the excitation of a parallel wire line by a distributed, in-phase constant amplitude current, over distances of many wavelengths, produces very little coupling. If a method could be found for stretching the guide wavelength by an order of magnitude or two, but only during a portion of the transmission line, considerably more excitation would occur.

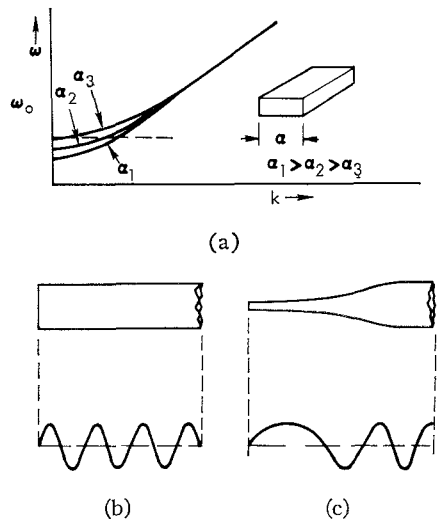

Fig. 6. (a) Dispersion curves for rectangular waveguide, for various widths. It is seen that at a constant frequency the wavenumber k (and therefore $\lambda=2\pi/k$) depends on the guide width. (b) Wavelength picture for a waveguide of uniform cross section. (c) Wavelength picture for guide of tapered width.

This possibility exists in the use of waveguides, where the guide wavelength is a function of the guide dimensions. By tapering a guide so that a portion is near "cutoff," while the rest of it is wide enough to be well in the propagating region of the ω-k diagram, a wavelength picture such as that of Fig. 6, is created. If this guide is excited with a uniform in-phase current density, or its equivalent, the "Net Dipole Moment" created in the section that is near "cutoff," where the wavelength is very long, would then increase the coupled voltage above the value J_0Z_0/k of (8).

The magnetic quantity that is the spin-wave analog of the waveguide "guide dimension" is H_i, for it controls the wave number at a given frequency. Therefore, a properly tapered magnetic field could produce a large effective Net Dipole Moment. As recognized by Schlömann, this tapered field exists automatically in specimens of nonuniform demagnetizing factor.

Experimental evidence of this method of the enhancement of spin-wave excitation has been given by Eshbach [11], Strauss [2], and Damon and van de Vaart [13]. We will now examine its applicability to the case of F-K wave excitation.

D. Excitation of F-K Waves by Net Dipole Moment Excitation

It is well known and can also be readily seen from the preceding discussion and from Fig. 1, line A–D, that exchange spin waves that are launched inside a material by the method of Net Dipole Moment travel toward the direction of the weaker magnetic field. If a rod of

YIG of parallel ends that are perpendicular to the axis is located in a uniform axial externally applied magnetic field H_{dc}, the internal field H_i increases from the ends towards the center. Consequently, as noted by Strauss [1], no spin waves are propagated along the rod, except for those that tunnel through the magnetic wall in the form of acoustic waves.

To see if an axially magnetized short rod will propagate F-K waves and if excitation is enhanced because of a possible Net Dipole Moment effect, we will now examine the wavelength distribution inside such a rod. We must first find the internal magnetic field distribution, and then obtain the k values.

We consider a rod of length h and square cross section $a \times a$, saturated by an applied axial magnetic field H_a. The internal magnetic field on the axis is then $H_i = H_a - H_d$, where H_d is the demagnetizing field, given by

$$H_{d\text{-oersteds}} = 4M_s \left\{ \int_0^a \int_0^a \frac{z\,dx'\,dy'}{[x'^2 + y'^2 + z^2]^{3/2}} + \left| \int_0^a \int_0^a \frac{(h-z)\,dx'\,dy'}{[x'^2 + y'^2 + (h-z)^2]^{3/2}} \right| \right\}. \quad (17)$$

(We note that for the case of a thin square disk, where $a \gg h$, we get $H_d = 4\pi M_s$). The field H_i has been plotted in Fig. 7 for a short rod having the dimensions specified there.

From the knowledge of the local magnetic field and the F-K portion of the ω-k plot of Fig. 1, or from (3), we obtain the value of k, at that local field, corresponding to the frequency of the wave in question.

Using this procedure, we have determined the distribution of k in the short rod of Fig. 7, for an applied field of $H_a = 900$ Oe, and for a signal frequency of 2075 Mc. (These conditions were chosen to allow F-K wave propagation through the crystal, with microsecond time delay.) Fig. 8(a) gives an approximate picture of guide wavelengths. To plot this figure, we computed the quantity sin kx, where k is the spatially varying wave number appropriate to the magnetic field in the rod at 2075 Mc. The corresponding group velocity is given in Fig. 8(b).

We can make the following observations:

1) The wavelengths are macroscopic, of the order of a millimeter, except for the region in the immediate center of the specimen.

2) A strong Net Dipole Moment effect exists, since the area under the first half cycle of Fig. 8(a) is approximately twice that of the second. Since this is equivalent to a net coupling length of about 0.5 mm, it should be possible to couple very effectively from electromagnetic to (F-K)-mode magnetostatic energy, and vice versa.

3) Because of the long wavelengths near the crystal ends, coupling will be further enhanced if the RF magnetic field is localized. No microscopic geometry is required here, however, for even the magnetic field that would surround an exciting wire of 0.010 inch (0.25 mm) in diameter would fall to one eighth the value at the wire surface within the first millimeter.

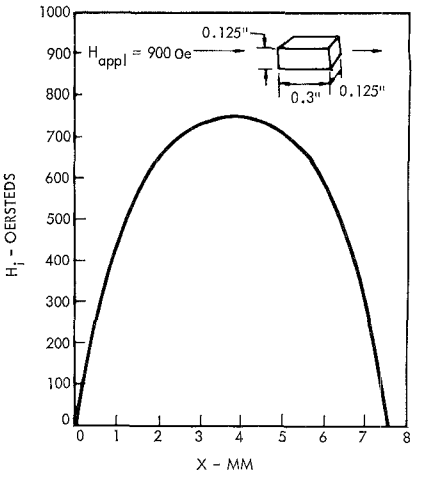

Fig. 7. Internal dc magnetic field along major axis of YIG specimen ($4\pi M_0 = 1750$ Oe) in an applied dc field of 900 Oe. Saturation of YIG parallel to axis is assumed.

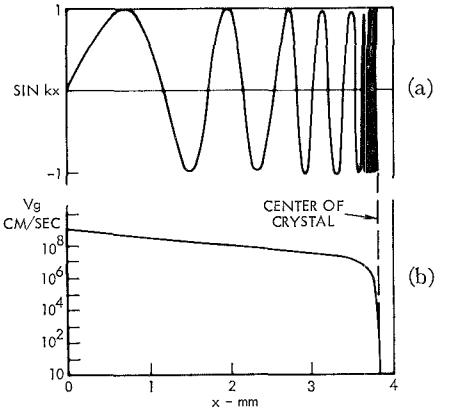

Fig. 8. Picture of wavelength and group velocity in left half of YIG specimen ($4\pi M_0 = 1750$ Oe) in applied H_{dc} of 900 Oe, at 2075 Mc, under the assumption of F-K wave propagation. An average radius of 0.19 cm is assumed here. The picture for the right half is the mirrow image. (a) Plot of the quantity sin kx, which gives a picture of the wavelength. (b) Group velocity.

4) Although the coupling between electromagnetic and magnetostatic wave fields will take place near the edge, the microsecond time delay will be due to the very narrow central region, where the field is at most within a few gauss of the cutoff value ($v_g = 0$).

5) The time delay occurs in the region where $k \simeq 2130$ cm^{-1}, so that the phase velocity $\omega/k \simeq (6)(10^6)$ cm/s. Since the group velocity for appreciable time delay is considerably smaller than this, a high degree of pulse dispersion is expected. This dispersion should get worse with reduction in group velocity and, therefore, with increases in time delay.

6) Since the long delay depends primarily on the group velocity in the center of the rod, the delay will change in a manner determined by H_i there. From Fig.

1, for H_i below "cutoff," as H_i is increased, v_g decreases; therefore, the time delay increases. As seen in Fig. 2, the change from $v_g = 10^6$ cm/s (1 μs/cm delay rate) to $v_g = 10^3$ cm/s (1000 μs/cm) occurs for a field variation of only a few oersteds.

IV. Experiments

A. Method of Observations

Experiments in which time delay caused by magnetic waves was observed have been described by several investigators. Our experiments, using the geometry treated in Section III-D, yielded a time delay of microwave pulses of two different types. Of these, the "low-field delay," to be described, was also found by Olson and associates [14], [15] and described at the 1964 PTG MTT International Symposium, at which our results were first described [16].

In all the experiments yet to be reported, short rods of single-crystal YIG[4] were immersed in an axial H_{dc} and excited with microwave power. Experiments in both the 1- and 2-Gc regions were performed. All tests were carried out at room temperature. To produce RF magnetic fields in the crystals, conductors short-circuiting RF transmission lines were placed adjacent to opposite surfaces, in the manner of Fig. 9, with one line connected to the input circuit, and the other to a microwave receiver. The circuit used in the tests is schematically shown in Fig. 10.

An overall picture of experimental results is given in Fig. 11. For this test, the crystal was of a square cross section ($\frac{1}{8}$ inch) and 0.3 inch long, with end faces ground parallel and polished. The short-circuiting conductors were 0.002-inch diameter copper wires. The receiver used was of high gain. (Unfortunately, however, its bandwidth was only 0.65 Mc, so that no faithful reproduction of 1-μs pulses could be expected.) The traces of Fig. 11, as well as those of the other series pictured, are photographically recorded observations of the signal detected by the receiver while the externally applied field H_{dc} was varied over a range of values, and the signal incident on the input coupling loop remained constant.

Referring to Fig. 11, we note that the upper trace of each frame has the same rectangular-shaped pulse. This is the video-detected input pulse. The pulse detected by the receiver is the negative-going pulse shown. At the high values of receiver gain used to obtain Fig. 11, a small amount of signal "leaked through" from input to output, so that a leakage pulse is shown in each frame.

We now focus our attention on the output signal, which has the following observed behavior:

1) At values of H_{dc} from 218 Oe, only a leakage pulse is transmitted, or, at least, a pulse that occurs at the same time as the leakage pulse.

[4] Purchased from Microwave Chemicals Lab., Inc., New York, N. Y.

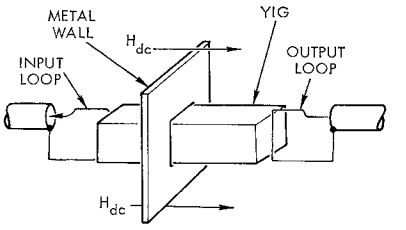

Fig. 9. Geometry for excitation of time-delayed signals. In some tests, the wire loop was replaced by a ribbon loop; in others, by an electric probe. The coaxial line was also replaced by a parallel wire line in some tests.

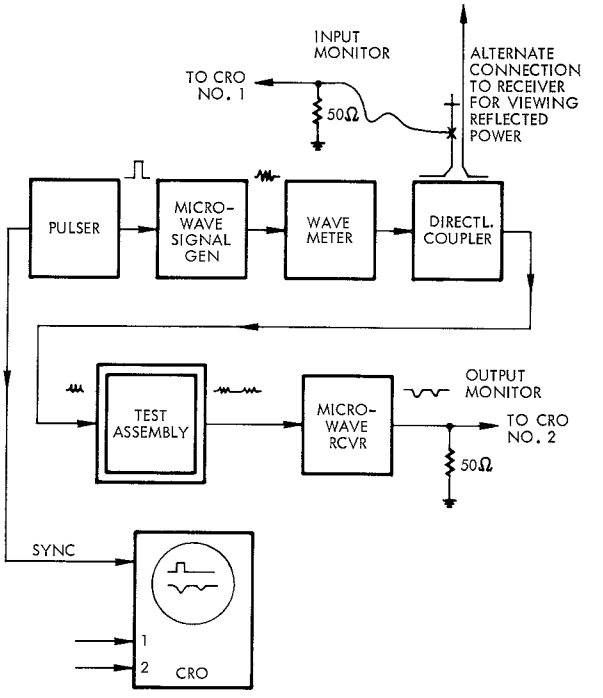

Fig. 10. Test circuitry for time delay experiments.

2) At several values of H_{dc}, such as $H_{dc} = 235$ Oe, the leakage pulse is distorted. This distortion is probably due to ferrimagnetic resonance absorption in a portion of the crystal.

3) In the very narrow range between 494 and 498 Oe, a time-delayed pulse appears. The delay interval increases from nearly zero to about 6 μs, for a field increase of only slightly more than 2 Oe. The width of the delayed pulse increases with delay, indicating that the delay line is highly dispersive. Furthermore, the amplitude of the delayed pulse decreases with time delay.

Additional discussion of these "low-field pulses" is given in Section IV-B. Continuing with the observations of Fig. 11, we find:

4) For fields from 534 to 1340 Oe, other delayed pulses are seen. These "high-field pulses" tune much more slowly with H_{dc} than the "low-field pulses." Furthermore, the delay here decreases as the magnetic field is increased while the pulse width remains approximately constant. A brief discussion of these "high-field pulses" is given in Section IV-C.

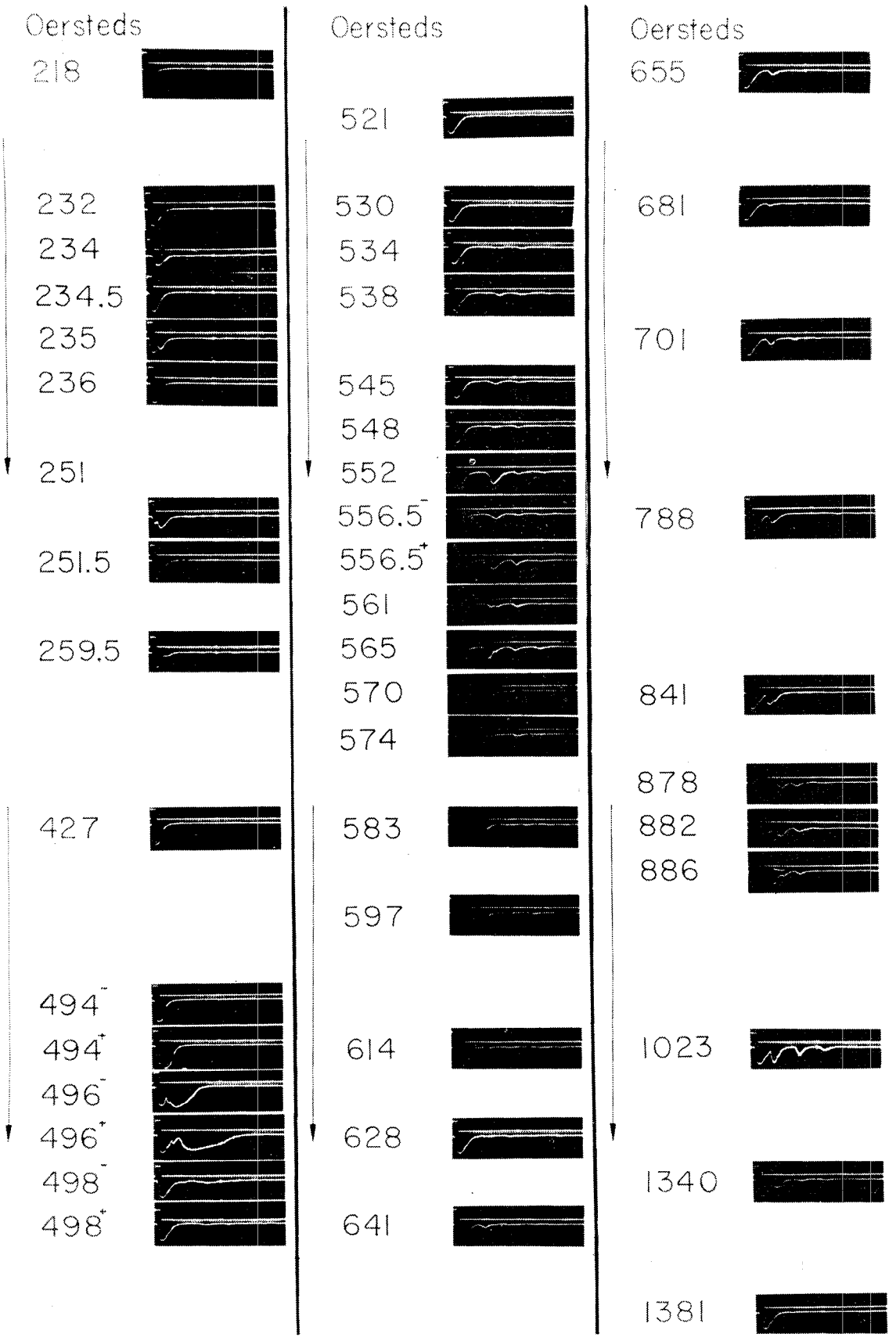

Fig. 11. Display of electronically variable delay of a microwave pulse. Frequency of microwave signal: 1230 Mc. Horizontal sensitivity: 2 μs/cm. (The length of an entire trace is 20 μs.) The number shown to the left of each frame is the applied H_{dc} at which the oscilloscope display of that frame was photographed. Time increases toward the right.

B. Low-Field Delay

A more detailed behavior of the "low-field delay" is given by the oscilloscope traces of Fig. 12, for H_{dc} varied through the immediate region of "low-field delay." These traces for a signal frequency of 2055 Mc were taken with a lower gain receiver system of 5 Mc bandwidth. The pulse shape and time delay shown are, therefore, more faithful reproductions of the envelope of the microwave signal.

Because of the lower gain, the ever-present leakage pulse of Fig. 11 is missing here. We do notice, however, that a very intense transmitted pulse, nearly coincident with the input pulse, exists at values of H_{dc} below those that produce delay. As H_{dc} is increased, this pulse separates from the input and becomes the delayed pulse.

The traces of Fig. 13, taken with the same setup as Fig. 12, demonstrate that the pulse delay is due to the propagation of a wave packet, for this figure shows both the transmitted pulse and that propagating back toward the source from the input loop (see Fig. 10). Here, the width of the initiating pulse was 0.66 μs, while the delay to the first pulse was 2 μs. Because of the dispersion which stretched the propagated pulses, a separation between input and reflected pulses was therefore not possible. The separation here is seen to be sufficient, however, to show the bouncing of a wave packet between input and output coupling zones; for, whenever the signal coupled to the output loop is a maximum, that coupled to the input loop is a minimum, and vice versa.

It was found that the "low-field signals" could just as easily be excited with unpolished as with polished rods. While the strongest excitation was obtained with H_{dc} parallel to the rod axis, somewhat weaker excitation was also found for H_{dc} perpendicular to the rod and exciting wire. The weakest excitation occurred when H_{dc} was perpendicular to the rod, but parallel to the exciting wire.

While, in most cases, excitation was with a 0.002-inch diameter wire short-circuiting the transmission line, effective excitation was also obtained with a thin copper strap short-circuiting the input transmission line and placed next to an end of a crystal, and with the extended inner conductor of an open-circuited line adjacent to an end.

The insertion loss varied from setup to setup. The lowest insertion loss at 2 Gc was obtained with loops short-circuiting the parallel wire transmission-line portion of baluns, at both ends. This loss was 24 dB, for a 1-μs delay. "Low-field delay" coupling was obtained both for rods that were uncoated, as well as for those whose sides (not ends) were coated with silver paint. The degree of coupling appeared to be equally strong for YIG rods of various orientations.

As expected, no coupling was observed with single-crystal manganese ferrite or polycrystalline ferrite, such as *R*-1 material.

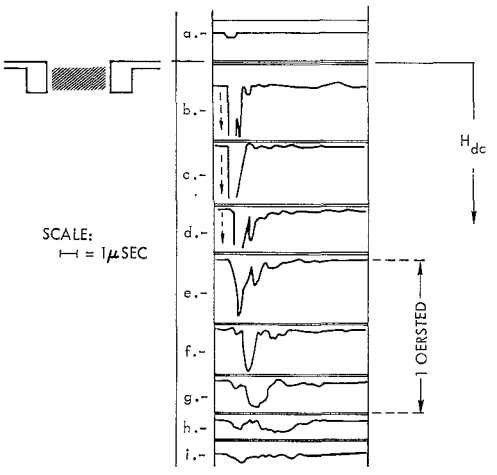

Fig. 12. Detailed behavior of "low-field delay" taken from CRO traces. Signal frequency: 2055 Mc. (a) Video-detected input pulse. (b)–(i) Output pulse seen as H_{dc} is increased in small increments through the region of "low-field delay." The change from (e) to (h) is approximately 1 Oe. Time increases toward the right. $H_{dc} \simeq 800$ Oe.

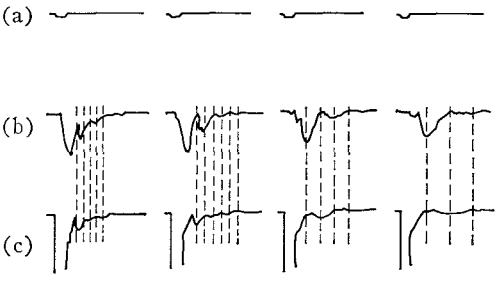

Fig. 13. Transmitted and reflected pulses for four values of increasingly higher values of H_{dc} (toward the right) in the "low-field delay" region, taken from CRO traces. Same arrangement as Fig. 12, (a) Video-detected input pulse. (b) Transmitted signal. (c) Reflected signal. Note that a maximum in transmitted signal corresponds to a minimum in the reflected signal, and vice versa. Time increases toward the right.

These "low-field delays" are surely magnetostatic waves, very closely related to *F-K* waves for the infinite rod,[5] for the following reasons:

1) Exchange-coupled spin waves cannot propagate through the axially magnetized rod; *F-K* waves can.

2) The minimum delay for *F-K* waves is $\sim 10^{-9}$ s/cm; so that a minimum-delayed pulse would appear coincident with the input pulse. Except for ~100-ns minimum displacement (probably caused by time response of the receiver, for it appears also on the leakage pulse), such a nearly-instantaneous response is seen here. Exchange-coupled spin waves would have a minimum delay of greater than 10 μs/cm.

[5] *F-K* refer to some preliminary experiments, by Fletcher, of pulse propagation in a ferrite cylinder, which may have been similar to ours. The conclusion that their waves were *F-K* waves was also reached by Olson and Yaeger [15].

3) The delay characteristics seen here follow those of the *F-K* mode. As H_{dc} is increased, coupled pulses with negligible delay (high v_g) are seen, until the region of critical H_{dc} is reached. Further increase of H_{dc}, by only a few oersteds, stretches the delay out to several microseconds.

4) The rather strong coupling of only 24-dB overall loss for 1-μs delay suggests a very efficient coupling mechanism, such as that discussed for *F-K* waves in Section III-D and Fig. 8.

5) The equally strong coupling obtained with several configurations of excitation (fine wire loop, thick wire loop, thin strip) suggests coupling into a wavelength picture as that of Fig. 8.

We recognize one difficulty that prevents complete correlation to date. From Fig. 2, long *F-K* time delays at 1230 Mc should occur at H_{dc} just below 439 Oe. When the applied field is 900 Oe, then for the $\frac{1}{8}$ inch by $\frac{1}{8}$ inch by 0.3 inch rod, the field at the center is 439 Oe. The applied H_{dc} measured at long time delays at this frequency was $\sim$494 Oe. With this H_{dc}, the specimen is not saturated. If it were, the field at the ends would have a sense opposite to that of the applied H_{dc}. Further work is planned to resolve this question. Additional work is also in order to explain the coupling that was observed for orientations of H_{dc} transverse to the rod axis.

C. High-Field Delay

Whereas the "low-field delay" appears due to *F-K* waves, the phenomenon of the "high-field delay" has not been completely explained. We will, therefore, merely list the following observations:

1) "High-field delay" pulses were seen only with a very sensitive receiver.

2) Several delayed pulses are visible in many frames of the traces.

3) As H_{dc} is increased, the delay slowly decreases.

4) To date we observed these pulses only with specimen having parallel optically polished ends.

It is probable that these pulses are of the same type as those observed in Strauss' reflection experiments [1], or related ones, that have crossed the magnetic wall in the center of the rod in some manner.

V. Conclusions

In this paper we have discussed some characteristics of magnetic waves, as applied to the time delay of microwave signals. These have included some microwave analogs of these waves, and some discussions relating to their excitation. Perhaps the major aspect of the paper, however, deals with microsecond-transit-time propagation through axially magnetized rods by signals that have the characteristics of Fletcher-Kittel magnetostatic waves. These waves can exhibit a very large Net Dipole Moment effect in coupling and, therefore, propagate through a rod with relatively low insertion loss. According to the *F-K* theory, the group velocity of these waves can be altered from nearly electromagnetic speeds to acoustic speeds, merely by changing H_{dc}. Our experimental work here has dealt only with the propagation at the lower speeds, where experimental behavior correlated well with these *F-K* waves. Further work is in order with these wave systems, for they could well be useful not only for electronically variable time delay of the order of a microsecond, but also for shorter delays, or for dispersive delays for alteration of signal shapes.

Acknowledgment

The major portion of this work was carried out at TRW Space Technology Labs. Some of the calculations and a considerable amount of the writing of this paper, however, were carried out while one of the authors, I. Kaufman, was a guest at the Centro Microonde, Florence, Italy, with a grant under the auspices of the Fulbright-Hays act.

It is a pleasure to acknowledge the work of D. Resman, in the preparation of the YIG crystals, and that of G. Komatsu, in the laboratory.

References

[1] Strauss, W., Magnetoelastic waves in yttrium iron garnet, *J. Appl. Phys.*, vol 36, Jan 1965, pp 118–123.
[2] ——, A new approach to high frequency delay lines, *IEEE Trans. on Sonics and Ultrasonics*, vol SU-11, Nov. 1964, pp 83–89.
[3] Auld, B. A., Walker modes in large ferrite samples, *J. Appl. Phys.*, vol 31, Sep 1960, pp 1642–1647.
[4] Herring, C., and C. Kittel, On the theory of spin waves in ferromagnetic media, *Phys. Rev.*, vol 81, Mar 1, 1951, pp 869–880.
[5] Clogston, A. M., et al., Ferromagnetic resonance line width in insulating materials, *J. Phys. Chem. Solids*, vol 1, 1956, p 129–136.
[6] Walker, L. R., Magnetostatic modes in ferromagnetic resonance, *Phys. Rev.*, vol 105, Jan 15, 1957, pp 390–399.
[7] Fletcher, P. C., and C. Kittel, Considerations on the propagation and generation of magnetostatic waves and spin waves, *Phys. Rev.*, vol. 120, Dec 15, 1960, pp 2004–2006.
[8] Damon, R. W., and J. R. Eshbach, Magnetostatic modes of a ferromagnetic slab, *J. Appl. Phys.*, vol 31, May 1960, pp 104S–105S.
[9] Schlömann, E., Spin wave spectroscopy, in *Advances in Quantum Electronics*, J. R. Singer, Ed. New York: Columbia University Press, 1961.
[10] ——, Generation of spin waves in nonuniform magnetic fields. I. Conversion of electromagnetic power into spin-wave power and vice versa, *J. Appl. Phys.*, vol 35, Jan 1964, pp 159–166.
[11] Eshbach, J. R., Spin-wave propagation and the magnetoelastic interaction in yttrium iron garnet, *J. Appl. Phys.*, vol 34, Apr 1963, pt 2, pp 1298–1304.
[12] Jacobsen, E. H., Sources of sound in piezoelectric crystals, *J. Acoust. Soc. Am.*, vol 32, 1961, p 949.
[13] Damon, R. W., and H. van de Vaart, Dispersion of long wavelength spin waves from pulse echo experiments, *Phys. Rev. Lett.*, vol 12, May 25, 1964, pp 583–585.
[14] Olson, F. A., and L. D. Buchmiller, A two-port microwave variable delay line, presented at 1964 Internat'l Symp., Long Island, N. Y.
[15] Olson, F. A., and J. R. Yaeger, Propagation, dispersion, and attenuation of backward-traveling magnetostatic wave in YIG, *Appl. Phys. Lett.*, vol 5, Jul 15, 1964, pp 33–35.
[16] Kaufman, I., and R. F. Soohoo, Properties and excitation of spin waves—A new microwave time-delay medium, presented at 1964 Internat'l Symp., Long Island, N. Y.